SAND2013-5025C

FULLY-KINETIC PARTICLE-IN-CELL SIMULATIONS OF TRIGGERED THREE-ELECTRODE GAS SWITCHES*

C. Thoma, D.R. Welch, D.V. Rose, W.R. Zimmerman, C. L. Miller, and R. E. Clark
Voss Scientific, LLC, Albuquerque, New Mexico

J. Schwarz, P. Rambo, M.E. Savage, and J.R. Woodworth
Sandia National Laboratory

* Sandia National Laboratories is a multi-program laboratory managed and operated by Sandia Corporation, a wholly owned subsidiary of Lockheed Martin Corporation, for the U.S. Department of Energy's National Nuclear Security Administration under contract DE-AC04-94AL85000.

Abstract

We present the results of 2D and 3D fully-kinetic electromagnetic particle-in-cell Monte Carlo (PICMC) simulations of triggered three-electrode gas switches using dry air as a gas (at pressures greater than 1 ATM). In such switches the AK gap voltage is set slightly below the breakdown threshold. A voltage pulse applied to a trigger needle placed in the AK gap allows breakdown to occur between, first, the trigger and anode, followed by the trigger and cathode. We demonstrate that a fully-kinetic PICMC approach can be used to follow the entire evolution of the switch, from the initial avalanche and streamer formation up to the fully conducting phase. We utilize an 18-species air chemistry model which is shown to agree with swarm parameters (breakdown threshold, drift velocity) obtained by experiment. Photon transport and photo-ionization are also included to permit the modeling of cathode directed streamers. This computational model will be used to help design closing switches for pulsed-power systems.

(1) Introduction and Outline

We describe the results of 2D and 3D hybrid-PIC simulations with the LSP [1] code of a **triggered three-electrode railgap closing switch** being designed and fielded at Sandia National Laboratory (SNL) for pulsed power applications.

These are **fully-kinetic** electromagnetic simulations of the switch using air as the working gas at a pressure of many atmospheres.

A high density gas is required to hold off a 200 kV voltage (for an AK gap of ~ 1 cm) until a pulse applied to the trigger electrode initiates a multi-step closing process.

Outline:

- Description of the operation of three-electrode railgap switch and introduction of switch geometry, driving circuits, and operating parameters.
- Description of 18-species air chemistry including photon generation and transport, and description of PICMC algorithms for kinetic particle-based chemistry modeling.
- 2D Cartesian railgap simulation results.
- 3D Cartesian railgap simulation results.
- Conclusions

(2) Schematic Operation of Three-Electrode Closing Switch

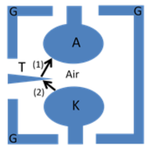

Schematic drawing of cross-section of three-electrode triggered closing switch. AK gap ~ 1.5 cm

The three electrodes are the cathode (K), anode (A), and trigger (T).

Prior to opening of switch A and K are held fixed potentials (e.g. +100 kV and 100 kV). The surrounding metal is held at ground (G) and T floats electrically.

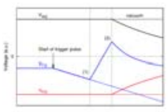

Schematic of electrode voltages as a function of time

The initial AK gap voltage must be small enough to hold off breakdown of the air.

But a voltage pulse applied to the trigger allows breakdown of the TA gap (1).

Due to TA gap current, the T voltage rises until the KT gap can break down. Resulting in a complete current path between A and K (2).

(3) Three Electrode "Railgap" Switch

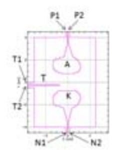

2D cross-section of railgap switch simulation space.

2D LSP simulation geometry for railgap switch in xy plane

P1,P2, etc. are open simulation boundaries which are connected to the circuits shown in the adjacent panel (4).

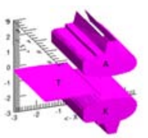

Full 3D geometry of railgap switch

Full 3D railgap geometry
For the full switch the "rail" electrodes extend in the z-direction for 12 cm (6 cm length shown here).

(4) Idealized Driving Circuits

Anode and cathode circuits:

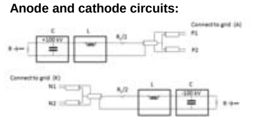

Trigger circuit

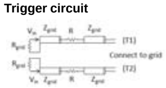

For a full 12 cm length railgap switch:
C = 80 nF
L = 60 nH
R_L = 2.1 Ω
R = 500 Ω

To avoid self-breakdown for V_{AK} = 200 kV and 1.5 cm AK gap requires an air density of 6.5 ATM

Railgap voltages in vacuum

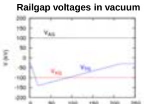

(5) LSP simulation of Railgap Switch

- We have performed 2D and 3D simulations of a railgap switch using the hybrid PIC code LSP [1].
- Fully-kinetic, PICMC treatment using 18 species air chemistry model. Includes O_2 attachment and photon generation and transport.
- Space-charge limited emission from trigger tip and cathode surface provides electron seed population.
- Adaptive particle management [2] with Eulerian remapping [3] used to keep particle number tractable during avalanche.
- Direct implicit field solution [4] and cloud-in-cell particle model [5] allows under-resolving electron plasma parameters.
- But time-step is constrained by need to resolve electron-neutral collision frequency.

(6) Air chemistry model

18 Total Species: e, N_2, O_2, Ar, N_2^+, O_2^+, Ar^+, N, N_4^+, O_2^-, O, O^-, O_4^+, NO^+, N^+, O^+, γ, N_2^*
where N_2^* is an excited state of N_2 (13.0 eV) which can radiatively relax and act as a source of photons.

Included Reactions:

1. Collisional ionization (including elastic and inelastic scattering)
   a) $e + O_2 \rightarrow e + e + O_2^+$
   b) $e + N_2 \rightarrow e + e + N_2^+$
   c) $e + Ar \rightarrow e + e + Ar^+$
2. Electron dissociation
   a) $e + O_2 \rightarrow O^- + O$
   b) $e + NO^+ \rightarrow N + O$
3. Electron attachment
   a) $e + O_2 + M \rightarrow O_2^- + M$
      i) $M = O_2$
      ii) $M = N_2$
   b) $e + O + O_2 \rightarrow O^- + O_2$
4. Charge exchange
   $N_2^+ + O_2 \rightarrow O_2^+ + N_2$
5. Formation and destruction of cluster ions
   a) $O_2^+ + O_2 + O_2 \rightarrow O_4^+ + O_2$
   b) $N_2^+ + N_2 + N_2 \rightarrow N_4^+ + N_2$
   c) $O_4^+ + N_2 \rightarrow O_2^+ + O_2 + N_2$
   d) $e + N_4^+ \rightarrow N_2 + N_2$
   e) $e + O_4^+ \rightarrow O_2 + O_2$
6. Electron-ion recombination
   a) $e + O_2^+ \rightarrow O + O$
   b) $e + N_2^+ \rightarrow N + N$
7. Detachment
   a) $O_2^- + M \rightarrow e + O_2 + M$
      i) $M = O_2$
      ii) $M = N_2$
   b) $O^- + O \rightarrow e + O_2$
8. Ion-ion recombination
   a) $N_2^+ + O_2^- \rightarrow N_2 + O_2$
   b) $O_2^+ + O_2^- \rightarrow O_2 + O_2$
9. Miscellaneous
   a) $N^+ + O_2 \rightarrow NO^+ + O$
   b) $O^+ + N_2 \rightarrow NO^+ + N$

(7) Scattering and Chemistry Reactions

Algorithms and Cross-sections

Reactions (1a), (1b), and (1c) are all modeled by standard PICMC methods [6] [7].

All cross-sections for these reactions are obtained from the cross-section database of the Boltzmann code EEDF [8].

Reactions (2)-(9) are modeled by the binary scattering algorithms described by Nanbu and Yonemura [9] [10].

Cross-sections for these reactions are obtained from the literature: (2a) [11], (2b), (3a), (3b), (8a), (8b), (9a), (9b) [12], (4), (5b), (5e), (6a), (6b), (7b) [13], (5a) [14], (5c), (7a): [15].

In many cases only the reaction rate, *k(T)*, is provided rather than the cross-section, which is needed for the kinetic PIC treatment.
In these cases were obtain the cross section as follows [16]:
If the reaction rate is given by

$$k(T) = k_o T^n \exp[-\Delta E / T],$$

then the center-of-mass cross-section, for any n > -3/2, can be written

$$\sigma(E) = \sqrt{\pi\mu/8}\,\frac{k_o}{\Gamma(n+3/2)}\,\frac{(E-\Delta E)^{n+1/2}}{E}\,\Theta(E-\Delta E).$$

(8) Cross-section plots

(1a): e-Ar

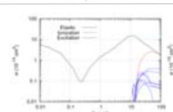

(1c), (2a): e-O_2

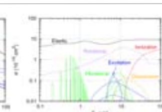

(1b): e-N_2

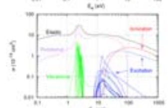

The N_2 excitation process with ΔE = 13.0 eV (dashed) is treated as a metastable species which generates photons (see Section 10).

Reactions (2)-(9):

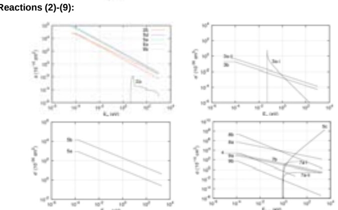

(9) Swarm Simulation Test of Air Model

Swarm simulations to test the air chemistry model:

- 1-cell PIC simulation with fixed applied electric field.
- Particle momenta are advanced but not particle positions.
- Particle self-fields are neglected.
- A seed electron population starts the avalanche.

At steady-state obtain transport parameters (usually functions of E/n for weakly-ionized plasma) .

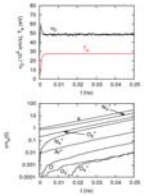

Sample swarm simulation:
Air at STP (78% N_2, 21% O_2, 1% Ar)
E/n =500 Td (1Td = 10^{-17} V-cm^2).
No photons.

Note:
1) There's no initial N^+ or O^+. This implies that you never get any, and consequently never get NO^+.
2) Density of O ~ density of O^-.
3) No N density because it can only be made be 2nd order reaction $e+N_2^+ \rightarrow N + N$.

Electron drift velocity and temperature go to steady-state values, and there is a constant ionization rate.

(10) Drift velocity and Ionization rate as a function of E/n for air:

Vary field for air at 1 ATM. Timestep chosen so that $\nu\Delta t$ ~ 0.1 where ν is the total electron-neutral collision frequency.

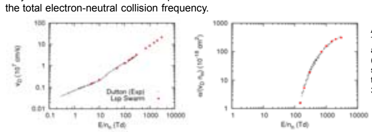

At 1 ATM for E/n < 120 Td, air becomes attachment dominated. (The critical field does not scale exactly as E/n, as the attachment process is 3-body)

Good agreement with experimental swarm data [17].

(11) Photon Generation and Transport

Photon generation:
We assume that one of the N_2 excited states (threshold 13 eV) is a metastable species.

$$e + N_2 \rightarrow e + N_2^*.$$

This state may then radiatively relax.

$$N_2^* \rightarrow N_2 + \gamma(13.0\ \text{eV}).$$

Relaxation is also treated in a Monte Carlo fashion with the relaxation probability each timestep given by $\Delta t/\tau_r$, where

$$\tau_r = \frac{\tau_o}{1 + P/P_o}.$$

For N_2, Yoshida and Tagashira suggest values of τ_o = 36 ns, and P_o = 60 Torr [18].

This process generates 13 eV photons.

Photon transport:
We then allow photo-ionization to occur:
$\gamma + X \rightarrow e + X^+$
where X = N_2, O_2, and O_2^-

For photons with E <13 eV, photo-ionization of N_2 is not possible

Photon transport algorithm of neutral atoms in Lsp is described by [3].
O_2^- absorption coefficient is given by Koopman [19].

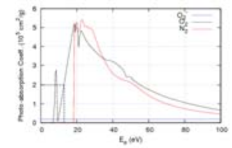

Photo-absorption coefficient of photons by O_2^-, O_2, and N_2. For 13 eV photons only photo-ionization by O_2 is significant.

(12) 2D Railgap Simulations

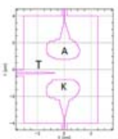

2D railgap switch simulation space. The switch is assumed to have a 1-cm extent in the virtual (z) direction.

- Initial AK voltage of 200 kV and 1.5 cm AK gap.
- Air at 6.5 ATM (n = 1.7x10^{20} cm^{-3}, T=273 K).
- Driving circuits and trigger pulse shown in section 4
- Circuit parameters are scaled to account for 1-cm length in virtual direction.
- Variable cell size, but $\Delta x = \Delta y$ = 400 μm in AK gap.
- Δt =3x10^{-5} ns (to resolve e-n collision frequency)
- ~10^5 total cells, > 10^7 particles.

Must be run for millions of timesteps.
~ 100 processors. Long runtimes (~ 1 week)

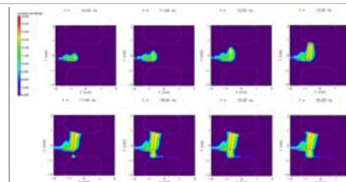

Ion density contours
Time evolution of switch closure:
~ 10 ns, streamer begins to form at trigger tip and propagate toward anode.
~ 13 ns, TA gap closes
~ 17 ns, streamer from cathode surface begins to propagate toward trigger.
~ 19 ns, KT gap closes and a full current path from K to A is established.

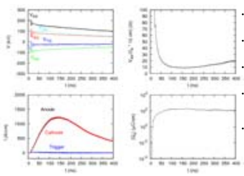

Time histories of 2D simulation.

- Some ringing when the switch begins to open.
- Negligible current leaks through trigger.
- Maximum current ~ 1200 A/cm.
- Minimum switch resistance ~ 10 Ω (for a 12-cm switch.)
- Switch resistance is inversely proportional to total electron charge.

(13) 3D Railgap Simulations

Problems with 2D results:

- Maximum electron density in 2D sim: 10^{16} cm^{-3}. Expect 1-2 orders of magnitude higher electron density.
- Maximum switch resistance in 2D sim: 10 Ω. Expect 1-2 orders of magnitude lower.

Motivation for 3D simulations:
In full a 3D railgap simulation we expect current filaments to form along the rails. Pinching of the filaments should produce higher current densities and more Joule heating which should lead to more ionization, and presumably higher electron densities and lower switch resistance.

3D Cartesian railgap simulation:

- Simulate only a 1.5-cm segment in the z-direction, and assume periodic boundaries. Edge effects are neglected.
- ~10^6 total cells, > 10^8 particles.

Must again be run for millions of timesteps.
On 100s of processors very long runtimes (~ 1 month).

Electron density iso-contours

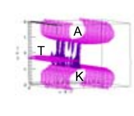

t= 16.2 ns, n_e = 2.2x10^{14} cm^{-3}

Density (and current) filaments are formed from both anode and cathode to trigger.

Electron density contours: cross-sections (t ~ 21 ns) along railgap shows filamentary structure

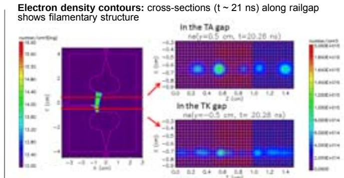

Squares show size of cells in xz plane (400x400 μm²)

Filaments are only a few cells in width. But simulations at higher resolution give same filament size.

Comparison of 2D/3D time histories

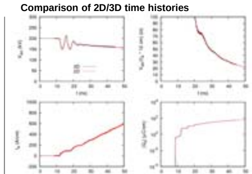

Despite presence of filamentary structure in 3D, the amount of charge and current per unit length are the same as 2D!

LSP simulations do not predict higher currents in 3D due to stronger pinching at higher dimensionality.

Conclusions

- We have performed 2D and 3D fully-kinetic hybrid-PIC simulations of the three-electrode triggered railgap closing switch.
- An air density of 6.5 ATM is required to hold off the 200 kV across the 1.5-cm AK gap until the switch is closed by a pulse applied to the trigger electrode.
- 2D and 3D simulations predict a total current of ~1.5 kA per unit length (along the rails). For a 12-cm length railgap this leads to a switch resistance on the order of 10 Ω. The electron number density in 2D and 3D reaches ~ 10^{16} cm^{-3}.
- 3D simulations show the development of longitudinal current filaments (radius ~1 mm, spacing ~ few mm). But there is no sign of enhanced current (or reduced switch resistance) due to three-dimensional pinching of filaments.
- These simulations qualitatively display closing switch behavior using a fully-kinetic PIC-based approach, but the electron densities are believed to be 1-2 orders of magnitude too small, and the switch resistance 1-2 orders of magnitude too large.
- We are currently investigating the possible causes of the low ionization state of the simulation results.

References

[1] LSP was developed by ATK Mission Research Corporation with initial support from the Department of Energy (DOE) SBIR Program.
[2] D. R. Welch, T. C. Genoni, R. E. Clark, and D. V. Rose, J. Comput. Phys. 227, 143 (2007).
[3] D. V. Rose, D. R. Welch, R. E. Clark, et al, Phys. Plasmas 18, 093501 (2011).
[4] D. R. Welch, D. V. Rose, M. E. Cuneo, R. B. Campbell, and T. A. Mehlhorn, Phys. Plasmas13, 063105 (2006).
[5] C. K. Birdsall and A. B. Langdon, "Plasma Physics Via Computer Simulation", Adam Hilger, New York, 1991.
[6] C. Birdsall, IEEE Trans. Plasma Sci. 19, 65 (1991).
[7] C. Thoma, T. P. Hughes, N. L. Bruner, T. C. Genoni, D. R. Welch, and R. E. Clark, IEEE Trans. Plasma Sci. 34, 910 (2006).
[8] A. Napartovich, "EEDF User's Guide", unpublished .
[9] K. Nanbu and S. Yonemura, J. Comput. Phys. 145 635 (1998) .
[10] K. Nanbu, Phys. Rev. E 55 4642 (1997).
[11] D. Rapp and D.D. Briglia, J. Chem. Phys. 43 1480 (1965).
[12] M. M. Campbell, et al, "IPROP User's Manual: Postprocessor Version" MRC Report MRC/ABQ-R-1397 (1991)
[13] M.N. Shneider et al, Phys. Plasmas 18, 063509 (2011)
[14] M.F. Danilov, Technical Physics 45, 21(2000).
[15] I.A. Kossyi et al, Plasma Sources Sci. Technol. 1, 207 (1992).
[16] S. H. Lin and H. Eyring , Proceedings of the National Academy of Sciences 68, 402 (1971).
[17] J. Dutton, J. Phys. Chem. Ref. Data 4, 557 (1975).
[18] K. Yoshida and H. Tagashira, J. of Phys. D, Appl. Phys 9, 491 (1976).
[19] D. W. Koopman, J. Appl. Phys. 44, 5328 (1973).